



Residual stress measurement by X-ray diffraction

Item Type	text; Thesis-Reproduction (electronic)
Authors	Chang, Yang-Ming, 1937-
Publisher	The University of Arizona.
Rights	Copyright © is held by the author. Digital access to this material is made possible by the University Libraries, University of Arizona. Further transmission, reproduction or presentation (such as public display or performance) of protected items is prohibited except with permission of the author.
Download date	23/08/2022 04:36:37
Link to Item	http://hdl.handle.net/10150/347810

RESIDUAL STRESS MEASUREMENT BY X-RAY DIFFRACTION

by

Yang-Ming Chang

A Thesis Submitted to the Faculty of the
DEPARTMENT OF METALLURGICAL ENGINEERING

In Partial Fulfillment of the Requirements
For the Degree of

MASTER OF SCIENCE

In the Graduate College

THE UNIVERSITY OF ARIZONA

1 9 7 2

STATEMENT BY AUTHOR

This thesis has been submitted in partial fulfillment of requirements for an advanced degree at The University of Arizona and is deposited in the University Library to be made available to borrowers under rules of the Library.

Brief quotations from this thesis are allowable without special permission, provided that accurate acknowledgment of source is made. Requests for permission for extended quotation from or reproduction of this manuscript in whole or in part may be granted by the head of the major department or the Dean of the Graduate College when in his judgment the proposed use of the material is in the interest of scholarship. In all other instances, however, permission must be obtained from the author.

SIGNED: _____

J. M. Chang

APPROVAL BY THESIS DIRECTOR

This thesis has been approved on the date shown below:

L. J. Demer

L. J. DEMER

Professor of Metallurgical Engineering

11 Aug. 1972

Date

ACKNOWLEDGMENTS

The author wishes to express his gratitude to his advisor, Dr. L. J. Demer, for his assistance and interest throughout this study. His guidance and understanding has made this work possible.

Thanks is also extended to Mr. H. F. Murray, whose help in the fabrication of the devices for this work was invaluable.

TABLE OF CONTENTS

	Page
LIST OF ILLUSTRATIONS	vi
LIST OF TABLES	viii
ABSTRACT	ix
1. INTRODUCTION	1
2. THEORETICAL BACKGROUND	4
2.1 Microstress and Macrostress	4
2.2 Elastic Stress-Strain Relations	7
2.3 Methods of Residual Stress Measurement by X-ray Diffraction	18
2.3.1 The Back-reflection Technique (Film Camera)	19
2.3.2 The Two-exposure Technique (Diffractometer)	25
2.4 Choice of Radiation and Filter	30
2.5 Location of Diffraction Peak	33
2.6 Factors Affecting the Intensity of the Diffraction Lines	35
2.7 Specimen Surface Treatment	39
3. OBJECTIVES	40
4. EXPERIMENTAL PROCEDURE	41
4.1 Specimen Preparation	41
4.2 Preparation of Special Devices	41
4.3 Residual Stress Studies	44
4.3.1 Two-exposure Method	44
4.3.2 Back-reflection Method	48
5. RESULTS AND DISCUSSION	56
5.1 Results	56
5.2 Discussion	57

TABLE OF CONTENTS--Continued

	Page
6. CONCLUSIONS	65
LIST OF REFERENCES	67

LIST OF ILLUSTRATIONS

Figure		Page
1	Effect of Lattice Strain on Debye-line Width and Position . . .	6
2	Pure Tension	8
3	Diffraction from Strained Aggregate, Tension Axis Vertical. Lattice Planes Shown Belong to the Same (hkl) Set. N = Reflecting-plane Normal'	10
4	Shear Stresses, τ , and Normal Stresses, σ , on an Element of Volume	13
5	Relation of Chosen Direction of Stress to Direction of Principal Stresses	15
6	Back-reflection Method at Normal Incidence	20
7	Back-reflection Method at Inclined Incidence	21
8	Schematic Showing Orientation of Measured Lattice Planes with Respect to Specimen Surface: (a) Specimen Normal to Beam, (b) Specimen Rotated ψ -Degrees	26
9	Use of a Diffractometer for Stress Measurement: (a) $\psi = 0$; (b) $\psi = \psi$	28
10	Absorption of X-rays in a 10-cm Path Length of Krypton and Argon, Each at a Pressure of 65 cm Hg	31
11	Parabola Fitted at Three Points to a Diffraction Peak . . .	34
12	Dimensions of Flat Tensile Specimens (a) Cu-20 w/o Zn, (b) Al-6061	43
13	Radially-adjustable Detector Support and Residual-stress Specimen Stage (Two Parts)	45
14	Uniaxial Straining Jig for X-ray Diffraction Stress Measurement Mounted on Specimen Stage, Aluminum Specimen Installed in Place	46

LIST OF ILLUSTRATIONS--Continued

Figure		Page
15	General Electric XRD-5 Diffractometer with Residual-stress Stage, Uniaxial Straining Jig, and Radially-adjustable Detector Support Installed: (a) $\psi = 0$, (b) $\psi = 30^\circ$	47
16	General Electric XRD-5 X-ray Unit with Pinhole Camera at Normal Incidence Exposure. Specimen Mounted in Position	49
17	Back-reflection Pinhole Pattern of Spot-welded Fin Specimen (Stress-free). Specimen-to-film Distance was 5 cm	51
18	Back-reflection Pinhole Pattern of Welded Spot No. 1 (57400 psi). Specimen-to-film Distance was 5 cm	52
19	Back-reflection Pinhole Pattern of Welded Spot No. 2 (-11900 psi). Specimen-to-film Distance was 3 cm	53
20	Back-reflection Pinhole Pattern of Welded Spot No. 3 (43000 psi). Specimen-to-film Distance was 5 cm	54
21	Back-reflection Pinhole Pattern of Welded Spot No. 4 (-1200 psi). Specimen-to-film Distance was 5 cm	55
22	Data for Stress vs Peak Shift, Cu-20 w/o Zn	58
23	Data for Stress vs Peak Shift, 6061 Aluminum Alloy	59
24	Schematic Drawing of Welded Spot Struck by the X-ray Beams	63

LIST OF TABLES

Table		Page
1	Distance from Center of Goniometer to Receiving Slit for Incidence Angles of 30° , 45° and 60° at Various 2θ Angles	29
2	Nominal Composition Limits, Weight Percent	42
3	Peak Shift for Cu-20 w/o Zn and 6061 Aluminum Alloy Stress Determinations	56
4	Values of Stress Factor, K, for 5083 Aluminum Alloy under Various Diffraction Conditions	60

ABSTRACT

The two-exposure X-ray diffraction method was used to make stress measurements on specimens of 6061 aluminum alloy and a Cu-20 w/o Zn alloy strained in tension on a special jig. SR-4 electric resistance strain gages applied to the specimens provided stress measurements for comparison with those obtained by X-rays. Closely linear data for peak shift vs stress level were obtained. Measured stress factors agreed closely with the results of other investigators.

Residual stress measurements were also made on small spot welds in an actual Inconel wing structure. In this case a film technique using a back-reflection method at normal incidence was employed. Reasonable stress values were observed.

CHAPTER 1

INTRODUCTION

One of the most important factors affecting the strength of a fabricated metal component is the presence of residual stresses, that is stresses which exist in the absence of external force. These are quite commonly found, especially in welded structures. Residual stresses play an important role in the mechanical behavior of materials such as fatigue, stress corrosion, and other mechanical and metallurgical phenomena. The modern, space age design of hardware requires a clear understanding of the origins and effects of residual stresses on mechanical behavior in order to control these stresses. To reach such an understanding requires accurate and reliable techniques for residual stress measurement.

A number of techniques have evolved for determining the state of stress in a body. These fall into two broad classifications, namely, destructive and nondestructive. Today the basic methods used for the measurement of residual stress are the X-ray diffraction and mechanical relaxation techniques (Cullity 1967). The X-ray diffraction technique is a nondestructive method which has found increasing application in the last few years. The mechanical relaxation technique is a destructive method which involves (a) removing part of the metal by cutting, grinding, etching, etc., and (b) measuring the change in shape or dimensions produced as a result of this removal.

The X-ray diffraction technique is strictly valid for the measurement of stress in a material which is elastic, homogenous, and

isotropic. Polycrystalline metals can generally be considered to a good approximation to satisfy these requirements (Christenson et al. 1960). Two general methods of measuring stress by X-ray diffraction which are now in use are the two-exposure technique (diffractometer) and the back-reflection technique (film camera). The two-exposure technique utilizing a diffractometer has received the widest application in the research and industrial fields. This is primarily because of its greater accuracy and speed. The relative stress determined by this method has been found to have a precision of the order of ± 3000 psi with annealed steel (Barrett and Massalski 1966).

The fundamental principle upon which the determination of stresses by X-ray diffraction techniques is based is that when the distance between atomic planes is altered, there is an accompanying change in the Bragg angle for X-ray diffraction. Therefore, when a metal is deformed elastically, the interplanar spacings change from their stress-free values to new values which are dependent on the magnitude and direction of the stress. These changes in spacings produce changes in the angles at which X-rays are diffracted by the planes. From the change in diffraction angle, which may be determined experimentally for some selected set of planes, it is possible to determine the stress in a given direction using the bulk elastic constants of the material or experimentally determined elastic constants obtained from X-ray diffraction measurements of the same material under known stress conditions.

The measurement of stresses by X-ray diffraction techniques has been well described in most textbooks on X-ray diffraction. The text,

Elements of X-Ray Diffraction (Cullity 1967) and the technical report, SAE TR-182 (Christenson et al. 1960), were the two major reference sources for this investigation.

The purpose of this present work was to study the measurement of residual stress in nonferrous metals. Specimens of a 6061 aluminum alloy and a Cu-20 w/O Zn alloy, both under tension conditions, were examined by the two-exposure method. SR-4 electric resistance strain gages were also applied to the specimens to provide comparison stress values. A spot-welded fin (INCONEL, 625, nickel-chromium alloy) specimen provided by the Hughes Aircraft Company was examined by the back-reflection film camera method.

CHAPTER 2

THEORETICAL BACKGROUND

2.1 Microstress and Macrostress

The measurement of residual stress by X-ray diffraction is actually a measurement of strain and not stress. The principal effect of residual stress is the distortion of the crystalline lattice. Such a distortion will change the spacing of the atomic planes. From Bragg's law:

$$n\lambda = 2d\sin\theta \quad (1)$$

where: $n = 1, 2, 3, \dots$

λ = wave length of X-ray beam in \AA ,

d = interplanar spacing of the diffracting planes,

θ = angle of incidence or reflection of X-ray beam.

It follows that a change, Δd , in the value of the interplanar spacing, d , while keeping the X-ray wave length constant, will alter or shift the diffraction angle θ by $\Delta\theta$. Thus differentiation of Bragg's equation yields

$$2\theta = -2(\Delta d/d)\tan\theta. \quad (2)$$

When a polycrystalline piece of metal is deformed elastically in such a manner that the strain is uniform over a relatively large distance the lattice plane spacings will change from the stress-free value to new values. Then the diffraction lines are shifted to new 2θ positions by the uniform macrostrain. On the other hand, if the metal is deformed plastically, the lattice planes usually become distorted in such a way

that the spacing of any particular (hkl) set varies from one grain to another or from one part of a grain to another. This nonuniform microstrain causes a broadening of the corresponding diffraction line, but the mean interplanar spacing is the same as in the unstrained condition (Cullity 1967).

The effect of strain, both uniform and nonuniform, on the direction of X-ray diffraction is illustrated in Figure 1. A portion of an unstrained grain is shown in (a) on the left, and the set of transverse reflecting planes shown has everywhere its equilibrium spacing d_0 . The diffraction line from these planes appears on the right. If the grain is then given a uniform tensile strain at right angles to the reflecting planes, their spacing becomes larger than d_0 , and the corresponding line shifts to lower angles but does not otherwise change, as shown in (b). This line shift is the basis of the X-ray method for the measurement of macrostress. In (c) the grain is bent and the strain is nonuniform; on the top (tension) side the plane spacing exceeds d_0 , on the bottom (compression) side it is less than d_0 , and somewhere in between it equals d_0 . This grain may be imagined to be composed of a number of small regions in each of which the plane spacing is substantially constant but different from the spacing in adjoining regions. These regions cause the various sharp diffraction lines indicated on the right of (c) by the dotted curves. The sum of these sharp lines, each slightly displaced from the other, is the broadened diffraction line shown by the full curve and, of course, the broadened line is the only one experimentally observable.

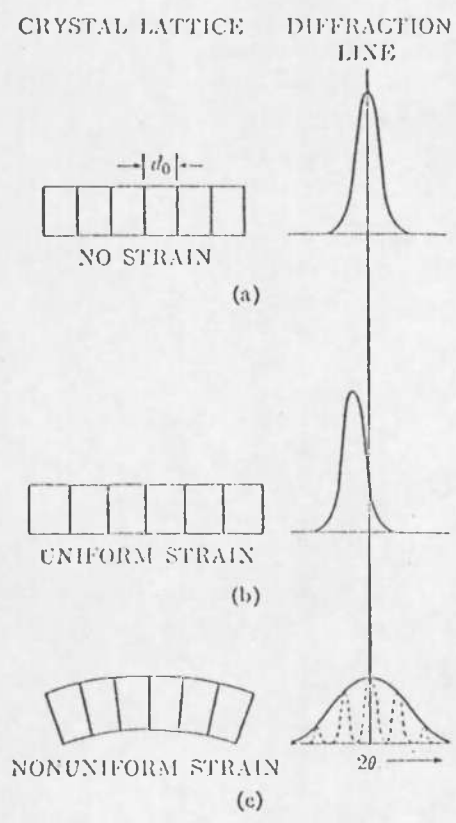


Figure 1. Effect of Lattice Strain on Debye-line Width and Position

Only elastic strain, not plastic strain, is indicated by the change in 2θ . This fact is useful in computing residual stresses from the measurements. In the X-ray diffraction method the strain gage is the spacing of lattice planes.

2.2 Elastic Stress-Strain Relations

The basic principles of the measurement of stresses by X-ray diffraction techniques are simple, and are based on measuring strain which is then converted to the stress by equations developed in the classical theory of elasticity. The X-ray method as described herein will detect elastic strain only, as the method is fundamentally a measure of inter-atomic spacings, which are altered by elastic stresses.

Consider a cylindrical rod of cross-sectional area A stressed elastically in tension by a force F shown in Figure 2. There is a stress $\sigma_y = F/A$ in the y -direction but none in the x - or z -direction. The stress σ_y produces a strain ϵ_y in the y -direction given by:

$$\epsilon_y = \frac{L_f - L_o}{L_o} = \frac{\Delta L}{L_o}, \quad (3)$$

where L_o and L_f are the original and final lengths of the bar.

Since the strain ϵ_y was produced by the stress σ_y , acting in the y -direction, Hooke's law states that the strain will be proportional to the stress that is:

$$\epsilon_y = \frac{\sigma_y}{E} \quad (4)$$

where E is Young's modulus. The elongation of the bar is accompanied by

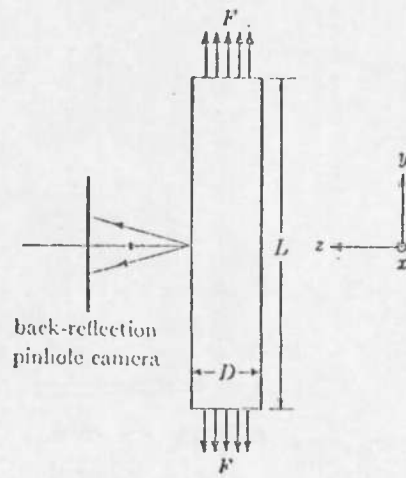


Figure 2. Pure Tension

a decrease in its diameter D . The strains in the x - and z -directions are therefore given by:

$$\epsilon_x = \epsilon_z = \frac{D_f - D_o}{D_o} \quad (5)$$

where D_o and D_f are the original and final diameters of the bar. If the material of the bar is isotropic, these strains are related by the equation

$$-\epsilon_x = -\epsilon_z = \nu \epsilon_y = \frac{\sigma_y}{E} \quad (6)$$

where ν is Poisson's ratio for the material of the bar. The negative signs denote contraction.

To measure ϵ_y by X-rays would require diffraction from planes perpendicular to the axis of the bar. Since this is usually physically impossible, we utilize instead reflecting planes which are parallel, or nearly parallel to the axis of the bar by taking a back-reflection photograph at normal incidence, as shown in Figure 2. In this way we obtain a measurement of strain in the z -direction:

$$\epsilon_z = \frac{d_n - d_o}{d_o} \quad (7)$$

where d_n is the spacing of the planes reflecting at normal incidence under stress, and d_o is the spacing of the same planes in the absence of stress. Combining Equations (4), (6), and (7), we obtain the relation:

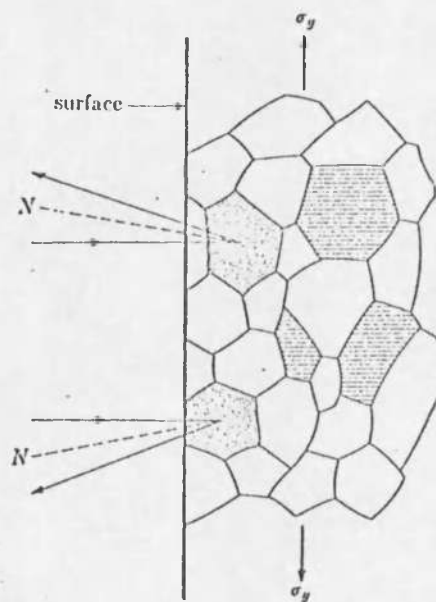


Figure 3. Diffraction from Strained Aggregate, Tension Axis Vertical.
Lattice Planes Shown Belong to the Same (hkl) Set.
N = Reflecting-plane Normal

$$\sigma_y = -\frac{E}{\nu} \left(\frac{d_n - d_o}{d_o} \right). \quad (8)$$

The above equation gives the required stress in terms of known and observed quantities.

It should be noted that only a particular set of grains contributes to a particular hkl reflection. These are grains whose (hkl) planes are almost parallel to the surface of the bar, as indicated in Figure 3, and which are compressed by the applied stress, that is, d_n is less than d_o . Grains whose (hkl) planes are normal to the surface have these planes extended, as shown in an exaggerated fashion in the drawing. The spacing d_{hkl} therefore varies with crystal orientation, and there is thus no possibility of using any of the extrapolation procedures to measure d_{hkl} accurately (Cullity 1967). Instead we must determine this spacing from the position of a single diffraction line on the film.

In a bar subject to pure tension the normal stress acts only in a single direction. But in general there will be stress components in two or three directions at right angles to one another, forming so-called biaxial or triaxial stress systems. However, the stress at right angles to a free surface is always zero, so that at the surface of a body, which is the place where we can measure stress, we never have to deal with more than two stress components and these lie in the plane of the surface. Only in the interior of a body can the stresses be triaxial.

Consider an infinitesimally small cube inscribed in the stress body and the cube edges are taken as coordinate axes, there will be, in general, three components of stress acting on each face, as shown in

Figure 4. Some of these will be equal if the cube is to be in a state of equilibrium.

Suppose we examine the cube face normal to the X axis. Across it we have the normal stress σ_x acting in the X-direction. We also have the two shearing stress, τ_{zx} , and τ_{yx} , the first subscript indicates in which axial direction the shear stress is acting, while the second subscript indicates the axis to which the plane of shear is perpendicular. Since under equilibrium conditions, $\tau_{yz} = \tau_{zy}$, $\sigma_x = \sigma_{-x}$, etc. Therefore, we require only six components of stress in order to specify completely the state of stress at a point in an isotropic solid, namely, σ_x , σ_y , σ_z ; τ_{xy} , τ_{yz} , and τ_{zx} .

A simplification results if the coordinate axes of Figure 4 are directed in such a way that the shear stresses on all faces are zero. This is always possible, regardless of the complexity of the stress system. The stresses normal to the cube surfaces are then the principal stresses σ_1 , σ_2 and σ_3 , and these are related to the principal strains ϵ_1 , ϵ_2 and ϵ_3 , in isotropic bodies by the equations:

$$\begin{aligned}\epsilon_1 &= \frac{1}{E}[\sigma_1 - \nu(\sigma_2 + \sigma_3)] \\ \epsilon_2 &= \frac{1}{E}[\sigma_2 - \nu(\sigma_1 + \sigma_3)] \\ \epsilon_3 &= \frac{1}{E}[\sigma_3 - \nu(\sigma_1 + \sigma_2)].\end{aligned}\tag{9}$$

Within the interior of the stressed specimen, each element of volume will, in general, be acted upon by three principal stresses, σ_1 , σ_2 and σ_3 , but at the surface, to which X-ray diffraction measurements

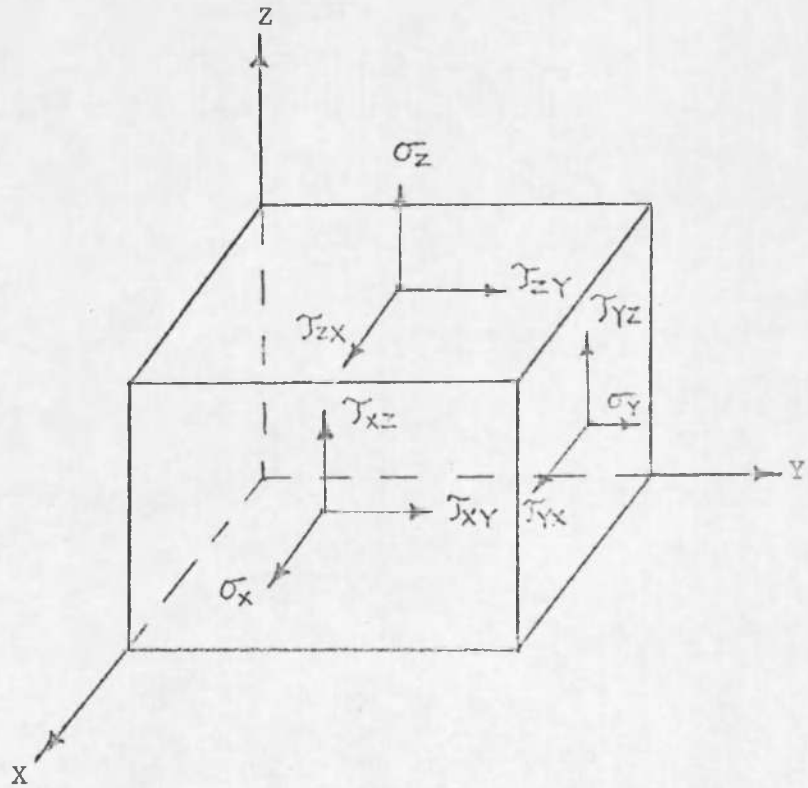


Figure 4. Shear Stresses, τ , and Normal Stresses, σ , on an Element of Volume

are confined, only two principal stresses, σ_1 and σ_2 lying within the plane of the surface are possible. The stress σ_3 which is normal to the free surface is zero, then:

$$\epsilon_3 = -\frac{\nu}{E}(\sigma_1 + \sigma_2). \quad (10)$$

The value of ϵ_3 can be measured by means of a diffraction pattern made at normal incidence and is given by Equation (7). Substituting this value into Equation (10), we obtain:

$$(\sigma_1 + \sigma_2) = -\frac{E}{\nu} \left(\frac{d_n - d_o}{d_o} \right). \quad (11)$$

The above equation relates the sum of the principal stresses to the change in d spacing. Its use is dependent upon the ability to measure the interplanar spacing in both stressed and unstressed conditions. The sum of the principal stresses is usually of little value to the engineer; furthermore, it may be impossible to obtain the same material in the unstressed state. A more useful quantity is the surface stress in a desired direction, which can be determined from two exposures of the surface. One measurement of the interplanar spacing is made with the X-ray beam normal to the surface of the specimen, and a second determination is made with the X-ray beam inclined at a known angle to the surface and lying in the vertical plane fixed by the surface direction of interest.

Consider that the stress σ_ϕ is desired at point 0 in the ψ direction of the specimen, as shown in Figure 5. It can be obtained from the photographs taken along the Z direction, and the ϕ direction. The

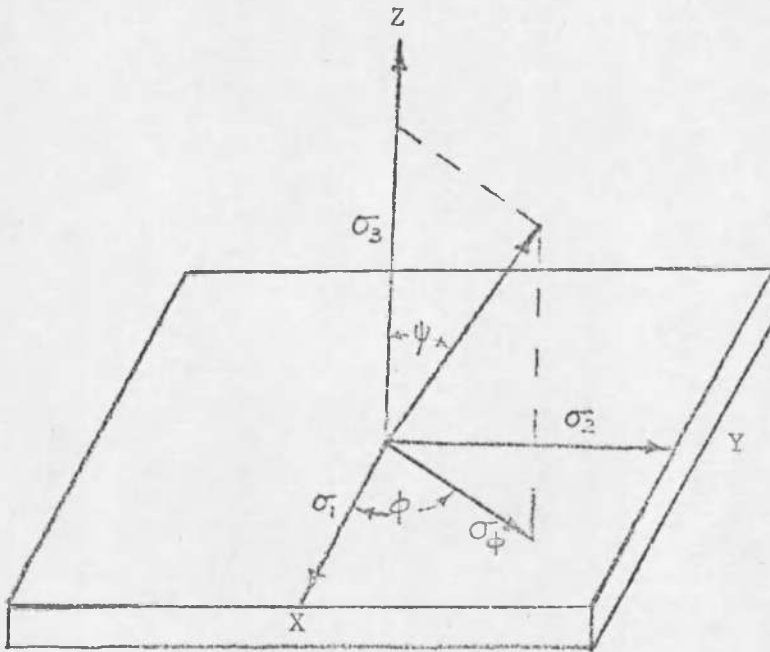


Figure 5. Relation of Chosen Direction of Stress to Direction of Principal Stresses

principal stresses σ_1 , σ_2 , and σ_3 are taken parallel to X, Y, and Z axes, respectively. The a_1 , a_2 , and a_3 are the direction cosines of the ψ direction relative to these axes. In terms of the angles ψ and ϕ , the direction cosines may be written:

$$\begin{aligned} a_1 &= \sin \psi \cos \phi \\ a_2 &= \sin \psi \sin \phi \\ a_3 &= \cos \psi = \sqrt{1 - \sin^2 \psi} \end{aligned} \quad (12)$$

Timoshenko (1936) derived the normal strain ϵ in any chosen direction as:

$$\epsilon = a_1^2 \epsilon_1 + a_2^2 \epsilon_2 + a_3^2 \epsilon_3. \quad (13)$$

Substituting the direction cosines in Equation (13) together with the values of the principal strains ϵ_1 , ϵ_2 , and ϵ_3 from Equation (9), and setting $\sigma_3 = 0$ (since the stress normal to a free surface is zero), then Equation (13) may be written:

$$\epsilon - \epsilon_3 = \frac{1 + \nu}{E} (\sigma_1 \cos^2 \phi + \sigma_2 \sin^2 \phi) \sin^2 \psi. \quad (14)$$

Now the normal stress σ in any chosen direction is given by:

$$\sigma = a_1^2 \sigma_1 + a_2^2 \sigma_2 + a_3^2 \sigma_3. \quad (15)$$

The stress parallel to the surface at ϕ degrees from the X axis is

$$\sigma_\phi = \sigma_1 \cos^2 \phi + \sigma_2 \sin^2 \phi. \quad (16)$$

Substitution of (16) in (14) gives the relation:

$$\sigma_{\phi} = (\epsilon - \epsilon_3) \cdot \frac{E}{1 + \nu} \cdot \frac{1}{\sin^2 \psi}. \quad (17)$$

Let d_0 be the spacing of atomic planes in the unstressed condition, d_{\perp} the spacing in the stressed condition perpendicular to the surface, and d_{ψ} the spacing in the direction specified by ψ, ϕ ; then

$$\epsilon - \epsilon_3 = \frac{d_{\psi} - d_0}{d_0} - \frac{d_{\perp} - d_0}{d_0} = \frac{d_{\psi} - d_{\perp}}{d_0}. \quad (18)$$

Since the interplanar spacing in the unstressed condition, d_0 , is not determinable in most cases, to a close approximation this may be written as:

$$\epsilon - \epsilon_3 = \frac{d_{\psi} - d_{\perp}}{d}. \quad (19)$$

Substituting Equation (19) into (17), the convenient equation form is obtained,

$$\sigma_{\phi} = \frac{d_{\psi} - d_{\perp}}{d_{\perp}} \cdot \frac{E}{1 + \nu} \cdot \frac{1}{\sin^2 \psi}. \quad (20)$$

Notice that the angle ϕ does not appear in this equation and fortunately so, since we do not generally know the direction of the principal stresses a priori; nor is it necessary to know the unstressed plane spacing d_0 . The measurement is therefore nondestructive, because there is no necessity for cutting out part of the specimen to obtain a stress-free sample.

When the measurement of stress is being conducted with a diffractometer, where in the position of the diffracted beam is measured in terms of the angular position, 2θ , it is convenient to write the stress equation (20) in terms of 2θ rather than plane spacings. Differentiating the Bragg law, we obtain:

$$\frac{\Delta d}{d} = \frac{\cot\theta \cdot \Delta 2\theta}{2} \quad (21)$$

Combining this relation with Equation (20) gives

$$\sigma_{\phi} = (2\theta_{\perp} - 2\theta_{\psi}) \cdot \frac{\cot\theta}{2} \cdot \frac{E}{1+\nu} \cdot \frac{1}{\sin^2\psi} \quad (22)$$

Where $(2\theta_{\perp} - 2\theta_{\psi})$ is expressed in degrees 2θ and

Let

$$K = \frac{\cot\theta}{2} \cdot \frac{E}{1+\nu} \cdot \frac{1}{\sin^2\psi} \cdot \frac{\pi}{180}$$

Then

$$\sigma_{\phi} = K \cdot (2\theta_{\perp} - 2\theta_{\psi}) \quad (23)$$

Where K is the stress factor, 2θ is the observed value of the diffraction angle in the normal measurement ($\psi = 0$) and $2\theta_{\psi}$ its value in the inclined measurement ($\psi \neq 0$). Since the stress factor K is directly proportional to the modulus, higher accuracies are attainable on materials having substantially lower elastic moduli, such as aluminum base alloys.

2.3 Methods of Residual Stress Measurement by X-ray Diffraction

Either the back-reflection technique (film camera) or the two-exposure technique (diffractometer) can be used for the measurement of

residual stress by X-ray diffraction. Each of these methods has its own advantages and limitations. Therefore, in making the decision as to which technique can best be employed for a particular problem, it is necessary to consider several factors. These include the purpose for which the stress information is needed, for this determines the precision with which the results must be obtained; the inherent precision of the several techniques; the errors introduced by the measuring process in each; and the time and effort needed to make an individual measurement. Another important consideration has to do with the type of specimen involved since this determines whether the alignment can be carried out easily and accurately in a laboratory environment or whether it is necessary to work under what might be called field conditions. Both methods are described in detail.

2.3.1 The Back-reflection Technique (Film Camera)

The back-reflection technique has some limitations such as less accuracy and speed, but it still plays an important role in the routine determination of residual stress in metals, particularly where heavy and bulky specimens are involved. The double-exposure technique (DET) is commonly employed in this method. The component of stress in any desired direction from plane spacings can be determined from two exposures, one made at normal incidence as shown in Figure 6 and the other with the incident beam inclined at an angle ψ to the surface normal, as shown in Figure 7. ψ is usually made equal to 45° . In this method, a powder of some reference material of known lattice parameter is smeared on the surface of the specimen for calibration purposes. The appearances of the

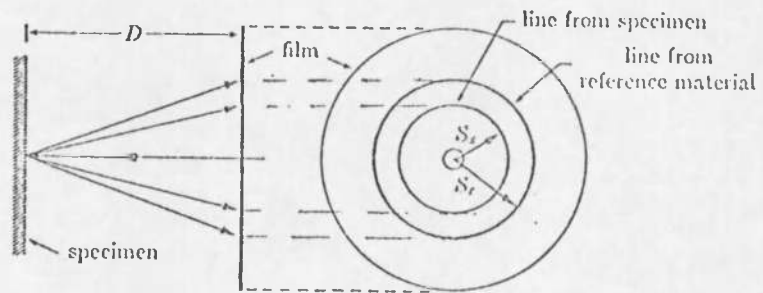


Figure 6. Back-reflection Method at Normal Incidence

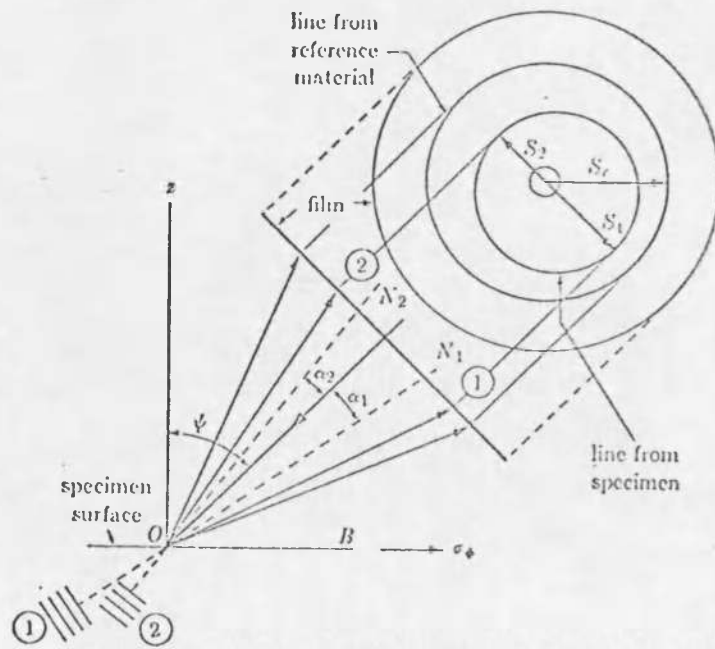


Figure 7. Back-reflection Method at Inclined Incidence

films are illustrated in Figure 6 and Figure 7. Since the line from the reference material calibrates the film, the plane spacings of the specimen are determined simply by measuring the diameters of the Debye rings from the specimen and from the reference material. The reference materials serve two purposes: first, they make accurate determination of the specimen-to-film distance possible; and second, they provide a reference for measuring diffraction line shifts from the stressed material. Annealed gold or silver powder is suitable for iron, aluminum, and brass, and annealed copper powder is good for nickel and its alloys.

Figure 7 shows that the Debye ring from the specimen is no longer perfectly circular. The reason lies in the fact that the strain along the normal to reflecting planes varies with the angle between these plane normals and the surface normal, as shown by Equation (17). There will therefore be slightly different diffraction angles 2θ for planes reflecting to the "low" side of the film (Point 1) and those reflecting to the "high" side (Point 2). These planes therefore form two sets of slightly different orientation, sets 1 and 2, having normals N_1 and N_2 at angles of α_1 and α_2 to the incident beam (α_1 and α_2 are nearly equal to one another and to $90^\circ - \theta$). Measurements of the specimen Debye-ring radii S_1 and S_2 therefore give information about strains in directions at angles of $(\psi + \alpha_1)$ and $(\psi - \alpha_2)$ to the surface normal. Cullity (1967) declared that in the usual practice S_1 is to be measured only, since the position of this side of the ring is more sensitive to strain.

To save time in calculation, Equation (20) can be put in more usable form. Since the Debye-ring radius S_1 in back reflection, is related to the specimen-to-film distance D by

$$\tan(180^\circ - 2\theta) = \frac{S}{D}$$

$$\text{or } S = D \tan(180^\circ - 2\theta) = -D \tan 2\theta, \quad (24)$$

$$S = -2D \sec^2 2\theta \Delta\theta.$$

Combining Equations (21) and (24), we obtain

$$S = 2D \sec^2 2\theta \tan \theta \cdot \frac{\Delta d}{d}.$$

Putting

$$\frac{\Delta d}{d} = \frac{d_\psi - d_\perp}{d_\perp},$$

then

$$\Delta S = S_\psi - S_\perp,$$

where S_ψ is the Debye-ring radius in the inclined-incidence photograph, usually taken as the radius S_1 in Figure 7, and S_\perp is the ring radius in the normal incidence photograph. Combining the last three equations with Equation (20), we obtain

$$\sigma_\phi = \frac{E(S_\psi - S_\perp)}{2D(1 + \nu) \sec^2 2\theta \tan \theta \sin^2 \psi}.$$

Letting

$$K' = \frac{E}{2D(1 + \nu) \sec^2 2\theta \tan \theta \sin^2 \psi},$$

then

$$\sigma_\phi = K'(S_\psi - S_\perp), \quad (25)$$

where K' is the stress factor which can be determined by tests made with known stresses applied to the particular material being studied.

In this method the pinhole camera is used and since the specimens to be examined are usually large and unwieldy, it is necessary to bring the camera to the specimen rather than the specimen to the camera. Since the highest accuracy is required in the measurement of diffraction line positions, the lines must be smooth and continuous, not spotty. This may be achieved by rotating or oscillating the film about the incident-beam axis. Complete rotation of the film is permissible in the normal incidence exposure, but not in the inclined incidence. In the latter case the Denye ring is noncircular to begin with, and complete rotation of the film would make the line very broad and diffuse. Cullity (1967) suggested that the film be oscillated through an angle of about 10° . If the specimen grain size is extremely coarse, the specimen itself should be oscillated if possible.

The component of stress can also be determined by the single-exposure technique (SET). In this technique the incident X-ray beam is directed toward the specimen surface at a fixed angle from the surface normal, and the diffracted beams corresponding to the two measuring directions which bisect the angle between the incident and diffracted beams are recorded simultaneously on two separate films or on the two sides of the same film. This method is less accurate than the double-exposure technique, but is quicker and simpler and makes less demands upon the skill of the operator (Norton 1968).

2.3.2 The Two-exposure Technique (Diffractometer)

The two-exposure technique has been widely used to determine residual stress in research and industrial applications. This method has a number of important advantages over the film method; the major ones are accuracy and speed. In this method, the desired component of stress in and parallel to the specimen surface is determined from two measurements, one with the diffractometer aligned in its normal position and the other with the specimen rotated at an angle ψ from its normal position. The rotation angle ψ most commonly used is 30° , 45° or 60° . An angle of 60° is about the practical maximum limit and in the interest of sensitivity of measurement an angle of ψ less than 45° is not desirable (Christenson et al. 1960). Figure 8 illustrates the orientation of the lattice planes to the sample surface and the direction of stress for the two positions. The component of stress to be determined can be related to the angular position 2θ of the diffraction beam by Equations (22) or (23)

$$\sigma_\phi = (2\theta_\perp - 2\theta_\psi) \cdot \frac{\cot\theta}{2} \cdot \frac{E}{(1+\nu)} \cdot \frac{1}{\sin^2\psi} \quad (22)$$

or

$$\sigma_\phi = K \cdot (2\theta_\perp - 2\theta_\psi), \quad (23)$$

where E = Young's modulus,
 ν = Poisson's ratio,
 K = Stress factor

$2\theta_\perp$ = the observed value of the diffraction angle in the "normal" measurement $\psi = 0$

$2\theta_\psi$ = the observed value of the diffraction angle in the inclined position $\psi = \psi$.

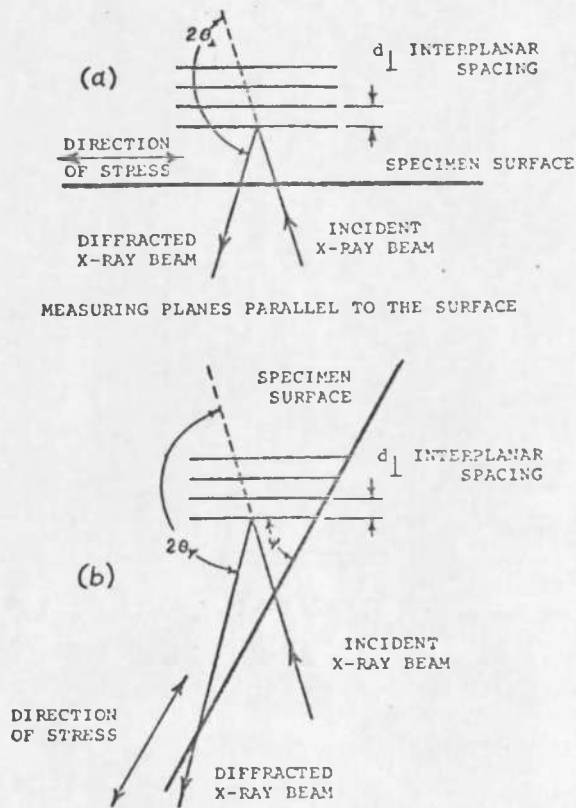


Figure 8. Schematic Showing Orientation of Measured Lattice Planes with Respect to Specimen Surface; (a) Specimen Normal to Beam, (b) Specimen Rotated ψ Degrees

Using this method, the only instrumental changes necessary are the addition of a specimen holder which will allow independent rotation of the receiving slit. This will be described in the later section.

The angular relationships involved in the diffractometer method were illustrated in Cullity (1967) as Figure 9. In (a), the specimen is equally inclined to the incident and diffracted beams; $\psi = 0$ and the specimen normal N_s coincides with the reflecting plane normal N_p . Radiation divergent from the source S is diffracted to a focus at F on the diffractometer circle. In (b) the specimen has been turned through an angle ψ for the inclined measurement. Since the focusing circle is always tangent to the specimen surface, rotation of the specimen alters the focusing circle both in position and radius, and the diffracted rays now come to a focus at F', located a distance r from F. The position of the receiving slit can be determined by

$$L = 5.73'' \times \frac{\cos[90^\circ - (\frac{2\theta}{2} - \psi)]}{\cos[(\psi + \frac{2\theta}{2}) - 90^\circ]}, \quad (26)$$

where

L = distance from center of goniometer to receiving slit in inches

5.73'' = machine design constant

ψ = specimen rotation angle

2θ = diffraction peak position.

The distance from center of goniometer to receiving slit in inches for incidence angles of 30° , 45° and 60° at various 2θ angles in increments of 2θ is tabulated in Table 1.

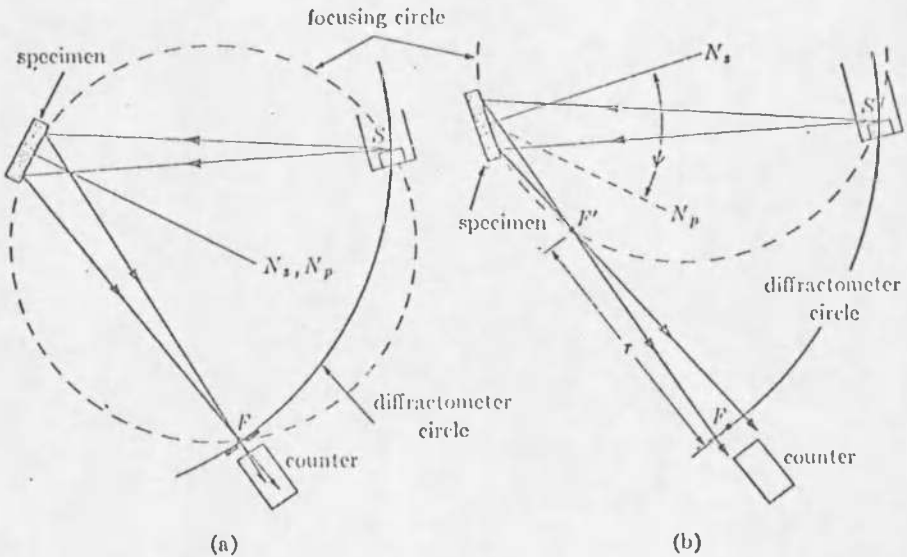


Figure 9. Use of a Diffractometer for Stress Measurement: (a) $\psi = 0$;
(b) $\psi = \psi$

Table 1

Distance from Center of Goniometer to Receiving Slit for Incidence Angles of
 30° , 45° and 60° at Various 2θ Angles

	$2\theta^\circ$	L"	$2\theta^\circ$	L"	$2\theta^\circ$	L"	$2\theta^\circ$	L"	$2\theta^\circ$	L"	$2\theta^\circ$	L"
PSI 30°	100	1.9	111	2.4	121	2.9	131	3.3	141	3.7	151	4.2
	101	2.0	112	2.5	122	2.9	132	3.3	142	3.8	152	4.2
	102	2.0	113	2.5	123	2.9	133	3.4	143	3.8	153	4.3
	103	2.1	114	2.6	124	3.0	134	3.4	144	3.9	154	4.3
	104	2.1	115	2.6	125	3.0	135	3.5	145	3.9	155	4.4
	105	2.2	116	2.6	126	3.1	136	3.5	146	4.0	156	4.4
	106	2.2	117	2.7	127	3.1	137	3.6	147	4.0	157	4.5
	107	2.2	118	2.7	128	3.2	138	3.6	148	4.1	158	4.5
	108	2.3	119	2.8	129	3.2	139	3.6	149	4.1	159	4.6
	109	2.3	120	2.8	130	3.2	140	3.7	150	4.1	160	4.6
	110	2.4										
PSI 45°	130	2.0	136	2.4	141	2.7	146	3.0	151	3.3	156	3.721
	131	2.1	137	2.4	142	2.7	147	3.1	152	3.4	157	3.792
	132	2.1	138	2.5	143	2.8	148	3.1	153	3.5	158	3.864
	133	2.2	139	2.6	144	2.9	149	3.2	154	3.5	159	3.938
	134	2.3	140	2.6	145	2.9	150	3.3	155	3.6	160	4.012
	135	2.3										
PSI 60°	150.00	2.0	151.75	2.2	153.50	2.4	155.25	2.5	157.00	2.7	158.75	2.919
	150.25	2.1	152.00	2.2	153.75	2.4	155.50	2.5	157.25	2.7	159.00	2.945
	150.50	2.1	152.25	2.2	154.00	2.4	155.75	2.6	157.50	2.7	159.25	2.970
	150.75	2.1	152.50	2.3	154.25	2.4	156.00	2.6	157.75	2.8	159.50	2.996
	151.00	2.1	152.75	2.3	154.50	2.5	156.25	2.6	158.00	2.8	159.75	3.022
	151.25	2.2	153.00	2.3	154.75	2.5	156.50	2.6	158.25	2.6	160.00	3.048
	151.50	2.2	153.25	2.3	155.00	2.5	156.75	2.7	158.50	2.8		

When the shape and size of the specimen permits, the two-exposure method is most often used to determine residual stress. The advantage of the direct-reading diffractometers over film in the measurement of diffuse lines occurs primarily from the fact that the contour of the diffuse diffraction line can be recorded accurately. This is influenced markedly by certain θ -dependent factors. Corrections for these factors, which will be shown later, are easily applied to the direct intensity measurements of the diffractometer and are difficult to apply to film blackening measurements. Another advantage to the use of diffractometers is the improvement in diffraction line contrast-peak to background. The X-ray absorption efficiency of krypton and argon, commonly used in X-ray counters, with respect to wave length is shown in Figure 10. This illustration, taken from Cullity (1967) indicates the superiority of krypton and argon for use with molybdenum and chromium or copper radiation, respectively. Further improvement is possible if a proportional or a scintillation counter is used with pulse-height discriminating circuits.

2.4 Choice of Radiation and Filter

The radiations usually employed in X-ray diffraction are the following:

Mo K_{α}	0.711 \AA
Cu K_{α}	1.542 \AA
Co K_{α}	1.790 \AA
Fe K_{α}	1.937 \AA
Cr K_{α}	2.291 \AA

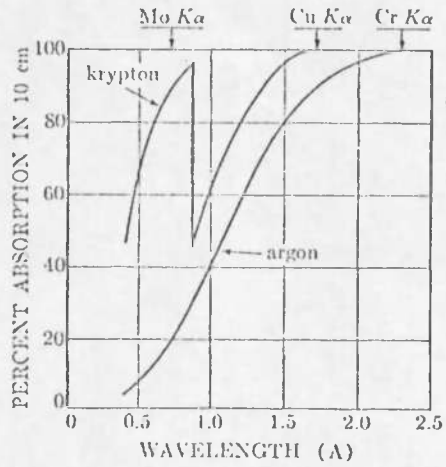


Figure 10. Absorption of X-rays in a 10-cm Path Length of Krypton and Argon, Each at a Pressure of 65 cm Hg

The Cu K_{α} radiation is generally the most useful, but it cannot be employed with ferrous materials since it will cause fluorescent radiation from the iron in the specimen. Instead, Co K_{α} , Fe K_{α} or Cr K_{α} radiation should be used. The rule-of-thumb for the choice of radiation is that the characteristic wavelength used should be longer than the K-absorption edge of the specimen, in order to prevent the emission of fluorescent radiation. In stress measurement the primary consideration in choosing a suitable radiation is to ensure that the wave length will provide a strong line at a sufficiently large diffraction angle so that adequate sensitivity of measurement is obtained. Another consideration is the degree of line contrast that may be achieved. This latter factor is particularly important in the measurement of diffuse lines. Line contrast can be improved by using a filter whose K absorption edge lies between the K_{α} and K_{β} wavelength of the target metal to absorb the K_{β} and the continuous spectrum. The filter is a material with an atomic number 1 or 2 less than that of the target metal. It was found that Cr K_{α} radiation with a 0.001"-thick vanadium foil filter provided good contrast between diffraction peaks and background radiation for the steel specimen. Using Cr K_{α} , the martensite (211) planes diffract at about $156^{\circ}(2\theta)$ and the 220 austenite line is available at 128° . Hilley, et al. (1966) suggested the use of Cr K_{α} , Co K_{α} or Cu K_{α} for stress measurements in aluminum and its alloys. Using Cr K_{α} , Co K_{α} , and Cu K_{α} , the (311), (420), and (511) (333) planes diffract at about 139.5° , 162.6° , and $162.5^{\circ} 2\theta$, respectively.

2.5 Location of Diffraction Peak

In stress measurement by X-ray diffraction it is necessary only to determine the angular 2θ shift in the lines upon angular ψ rotation of the sample with respect to the primary beam. Since small errors in $2\theta_{\perp}$ and $2\theta_{\psi}$ may have an appreciable effect on $(2\theta_{\perp} - 2\theta_{\psi})$, these angles must be measured with an accuracy of 0.02° or 0.03° (Christenson et al. 1960). If the lines are sharp it is relatively easy to measure such a shift, but if the lines are broad, an accurate measurement becomes more difficult. Fortunately, this difficulty can be overcome by Ogilvie's parabola-fitting method (Ogilvie 1952) whereby five data points are obtained at equal 2θ intervals about the intense region of the diffraction peak, and the parabolic curve is fitted by the method of least squares. A method which involves simpler computations and less measuring time by fitting a parabola to only three points has been developed by Koistinen and Marburger (1959). When the three data points chosen are restricted to points having intensities at least 85% of the maximum intensity and they straddle the peak of the diffraction curve, some lack of symmetry can be tolerated and the parabola will usually be a good approximation. Figure 11 shows three such measurements fitted to a parabolic curve. The position on abscissa of the vertex of the parabola is given by:

$$h = x_1 + \frac{c}{2} \cdot \frac{(3a + b)}{(a + b)} \quad (27)$$

where h = position on abscissa of vertex of parabola,

x_1 = position of first data point,

c = interval in X between data points,

a and b = difference in vertical coordinate (Y) between middle data point and data points on either side of it.

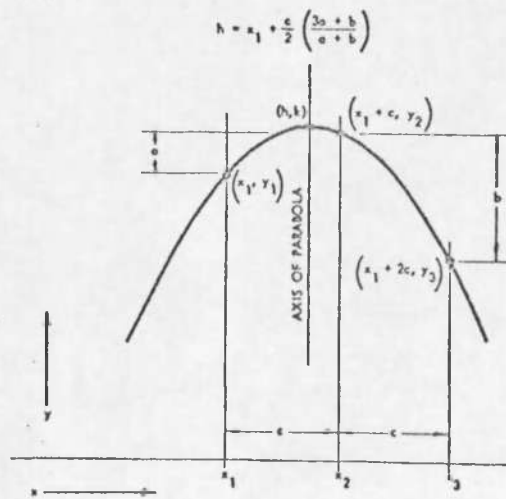


Figure 11. Parabola Fitted at Three Points to a Diffraction Peak

The parabolic method depends primarily on how well the diffraction peak is represented by a single parabola, that is, on the line symmetry. However, a little asymmetry is introduced into every diffraction line by certain θ -dependent intensity factors entering into the diffraction and measuring process. These intensity factors vary sufficiently slowly with θ that ordinarily they are of interest only in the variation in intensity of one line to another. In the special case of diffuse lines, however, the lines extend over a sufficient 2θ range that these factors markedly affect the line contour and apparent position. Hence, all broad line intensity measurements must first be corrected for these factors before a relative position is assigned to the line by fitting a parabola to the data.

2.6 Factors Affecting the Intensity of the Diffraction Lines

The factors which affect X-ray diffraction line intensity are known as the Polarization, Lorentz and absorption factors.

The Polarization factor, $1/2(1 + \cos^2 2\theta)$, comes from the Thomson equation (Cullity 1967)

$$I = I_0 \frac{e^4}{r^2 m^2 c^4} \left(\frac{1 + \cos^2 2\theta}{2} \right)$$

(where I = the total scattered intensity, I_0 = intensity of the incident beam, e = electron charge, m = mass of electron, r = scattered distance from the electron, c = velocity of light) for scattering by an electron because the incident beam is not polarized. The Thomson equation shows that the scattered intensity decreases as the inverse square of the

distance from the scattering electron, and that the scattered beam is stronger in forward or backward directions than in a direction at right angles to the incident beam.

The Lorentz factor

$$\frac{1}{4(\sin^2\theta\cos\theta)}$$

arises from certain geometrical considerations. The total integrated intensity of a reflection from a given family of planes is characteristic of the specimen material. However, the film or counter tube aperture at any one 2θ position, receives only a portion of this total integrated intensity which depends on the experimental arrangement. In most usage, the Lorentz and Polarization factors are combined, thus:

$$\text{Lorentz-polarization factor} = \frac{1}{8} \cdot \frac{1 + \cos^2 2\theta}{\sin^2 \theta \cos \theta} \quad (28)$$

Values of this factor are tabulated by Christenson et al. (1960).

The absorption factor is also a geometrical factor. This factor is quite important when the mean path length of the X-rays within the sample varies with the angle of diffraction. The usual diffractometer is so arranged that the sample surface, or the tangent to the sample surface, is at equal angles with the incident and diffracted beams ($\psi = 0^\circ$). This makes the path length and hence the absorption constant and independent of the angle θ . However, for a specimen angle ψ other than zero, the absorption becomes a function of the diffraction angle θ

and the diffracted intensity varies by $I_d = K(1 - \tan\psi \cot\theta)$. The derivation of this relation can be found in TR-182 (Christenson et al. 1960). It should be noted that the particular relationship derived does not apply to the common film techniques. The absorption factor for ψ angles of 30° , 45° , and 60° was tabulated by Christenson et al. (1960). The measured intensities are corrected for absorption by dividing the intensity measured at each angle of 2θ by the absorption factor for the 2θ angle. Christenson pointed out that it is unnecessary to correct the measured line intensities for background. This is fortunate since there is yet no simple method for properly correcting for background.

A simple and useful method for correcting the measured X-ray intensities by the use of the computed values for absorption and Lorentz-polarization factors and fitting a parabola to three points on the diffraction peak has been developed by Koistinen and Marburger (1959). This method provides the most rigorous approach and is believed to represent the best compromise between speed and accuracy of measurement. To simplify the correction procedure for angles of ψ other than zero, the absorption and Lorentz-polarization factors were combined into a single correction factor, as tabulated for three angles of ψ , by Christenson et al. (1960). When ψ is zero degrees, the absorption does not vary with 2θ , and the only correction to be applied is the Lorentz-polarization factor. It should be noted that the effect of the Lorentz-polarization factor is independent of the angle ψ , and, therefore, does not result in any apparent line shift upon rotation of the sample from the ψ equals zero degrees position to an angle of ψ other than zero. The absorption factor

is the only factor that causes a change in line symmetry and apparent line shift upon change of angle. However, in the fixing of relative line position by any method, such as the parabolic, which depends for its accuracy upon the degree of diffraction peak symmetry, it is wise to apply the corrections for the Lorentz-polarization effect since this correction is expected to improve line symmetry.

The X-ray diffraction intensity can be measured by both rate meter and scaler circuits provided by most modern diffractometers. The rate meter, the output of which is automatically recorded as a function of the diffraction angle, provides a more or less instantaneous average of the diffraction intensity. The scaler circuit permits either the accumulation and measure of the total number of X-ray counts or photons for a given interval of time or the measure of time required to accumulate a given number of counts. The former is known as fixed-time scaling and provides a direct measure of X-ray intensities. The latter is fixed-count scaling and results in the measure of inverse intensities. In the measurement of diffuse lines, the output of the rate meter is neither sufficiently accurate nor sufficiently sensitive for stress determination. Scaling must be used and fixed-count scaling is the better technique, since it enables the choice and use of a constant probable error.

The measured inverse intensities are corrected for factors sensitive to 2θ by multiplying the inverse intensities by the appropriate factors. Lorentz-polarization factors are used to correct the data obtained at zero degrees and the combined Lorentz-polarization-absorption

factors are used at angles of other than zero. After the points have been corrected the position of the vertex of the parabola given by Equation (27) may be rewritten as

$$2\theta_{\text{vertex}} = 2\theta_1 + \frac{c}{2} \left(\frac{3t_1 - 4t_2 + t_3}{t_1 - 2t_2 + t_3} \right), \quad (29)$$

where

t_1 , t_2 , and t_3 = time required to accumulate a given number of counts at $2\theta_1$, $2\theta_2$, and $2\theta_3$.

$2\theta_1$, $2\theta_2$, and $2\theta_3$ = consecutive 2θ positions at which inverse intensity is determined.

$$c = 2\theta_2 - 2\theta_1 \text{ or } 2\theta_3 - 2\theta_2$$

2.7 Specimen Surface Treatment

The penetration of the X-ray beam into the metal surface is very low and the X-rays are diffracted from surface layers only. Therefore, for reliable stress measurement the correct specimen surface treatment is extremely important. Surface roughness must be strictly avoided, because the points in a rough surface are not stressed in the same way as the bulk of the material and yet they contribute most to the diffraction pattern, especially the one made at inclined incidence. The specimen surface must be clean and smooth, but any mechanical procedure for cleaning or smoothing the surface will at least superficially disturb it and render it unfit for stress measurement by X-rays unless the disturbed layer is removed. Electropolishing or chemical etching may be the satisfactory method for smoothing or taking off stock.

CHAPTER 3

OBJECTIVES

The objectives of this investigation were as follows:

1. To become familiar with the two-exposure method and the back-reflection method for stress determination by X-rays, and to use them in tensile specimens of 6061 aluminum alloy and a Cu-20 w/o Zn alloy, and a spot-welded fin specimen of Inconel.
2. To design and fabricate the residual-stress specimen stage, radially-adjustable detector support, and the straining jig devices required for the diffractometer method.
3. To evaluate and compare stress measurements obtained by the X-ray diffraction method with those by the SR-4 electric resistance strain gage technique.

CHAPTER 4

EXPERIMENTAL PROCEDURE

4.1 Specimen Preparation

The materials used in this investigation were 6061-T6 aluminum alloy, Cu-20 w/o Zn, and a spot-welded aircraft fin (INCONEL,625 nickel chromium alloy) obtained from the Aluminum Company of America, the American Smelting and Refining Company, and the Hughes Aircraft Company, respectively. The nominal chemical composition of these materials in weight percent, as supplied by the producers, is given in Table 2. The flat tensile specimens of 6061-T6 aluminum alloy and Cu-20 w/o Zn were machined to the form shown in Figure 12. The specimens were given a metallurgical polish, and a 5% hydrofluoric acid solution was utilized to remove all smeared material from their surfaces. Then, they were annealed in a 95% nitrogen plus 5% hydrogen atmosphere at 345°C for one hour (6061-T6 aluminum alloy), at 400°C for one hour (Cu-20 w/o Zn) and cooled inside the furnace to relieve any mechanical stresses. To prevent any change of the original stressed condition from the spot welds, acetone was used to clean the surfaces of the spot-welded fin specimen.

4.2 Preparation of Special Devices

For the determination of residual stress by the two-exposure method, some special devices--residual stress specimen stage, radially-adjustable detector support, and straining jig were required. The first two were designed following types previously sold by the General Electric

Table 2

Nominal Composition Limits, Weight Percent

<u>Material</u>	<u>Si</u>	<u>Fe</u>	<u>Cu</u>	<u>Mn</u>	<u>Mg</u>	<u>Cr</u>	<u>Zn</u>	<u>Ti</u>	<u>Al</u>	
A1-6061	0.40-0.80	0.7	0.15-0.40	0.15	0.80-1.20	0.15-0.35	0.25	0.15	Balance	
Cu-20 w/o Zn	<u>Fe</u> 0.05	<u>Cu</u> 78.5-81.5	<u>Pb</u> 0.05	<u>Sb</u> 0.001	<u>Sn</u> 0.001	<u>Zn</u> Remainder				
Ni-Cr 625	<u>Si</u> 0.50	<u>Fe</u> 5.0	<u>Cr</u> 20.0-23.0	<u>Ti</u> 0.40	<u>Al</u> 0.40	<u>Co</u> 0.50	<u>Mo</u> 8.0-10.0	<u>Ni</u> Balance	<u>C</u> 0.10	<u>S</u> 0.015

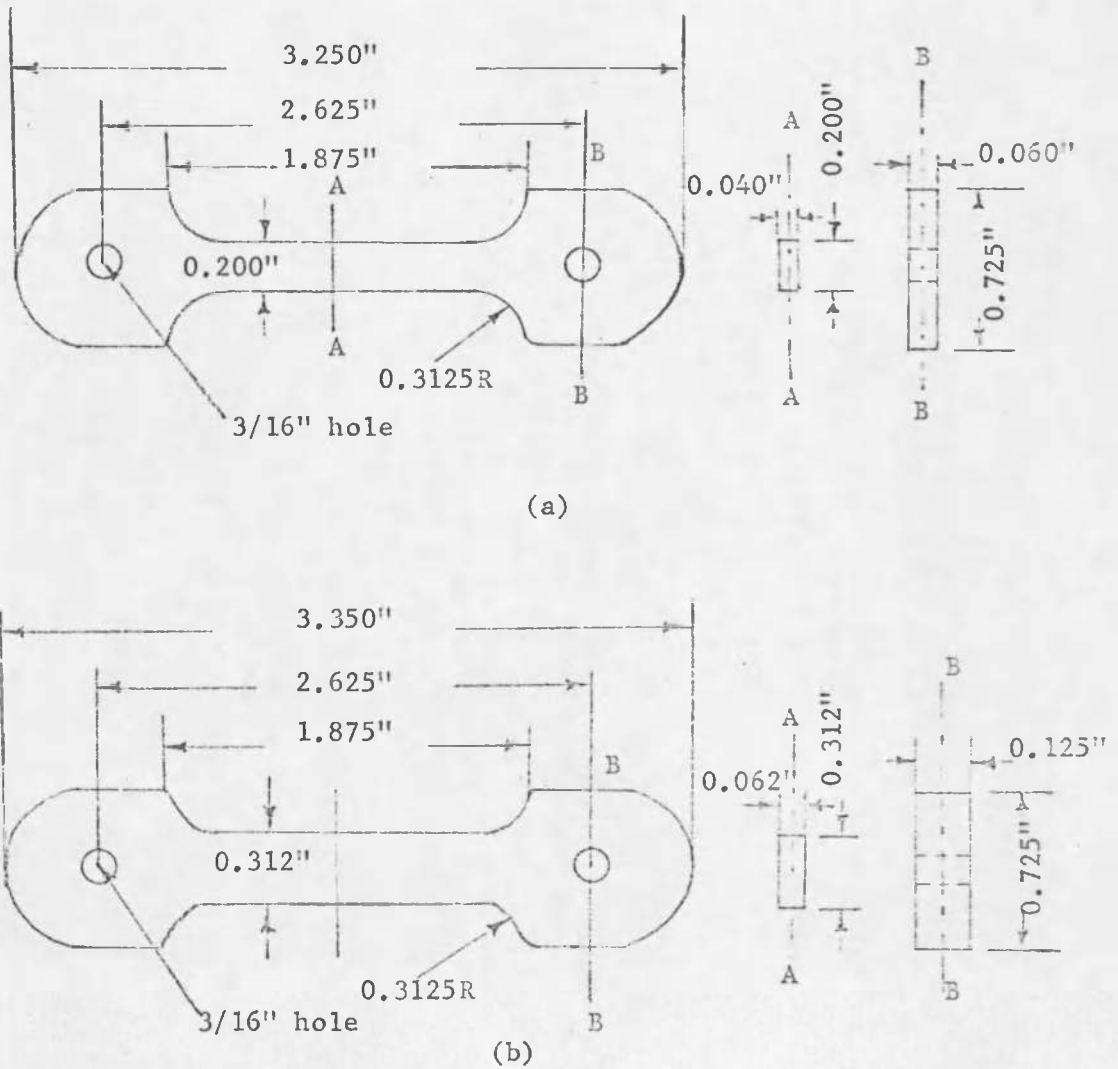


Figure 12. Dimensions of Flat Tensile Specimens (a) Cu-20 w/o Zn, (b) Al-6061

Company. The straining jig was patterned after one used by Hilley et al. (1967). These were constructed in the College of Mines shop. Photographs of the devices are shown in Figures 13 and 14. The residual stress specimen stage permits specimen rotation (ψ angle) about its vertical axis which coincides with the theta axis. The radially-adjustable detector support is used to adjust the receiving slit to a position which corresponds with the ψ angle rotation. The straining jig provides for applying a uni-axial tension load to the specimen.

4.3 Residual Stress Studies

4.3.1 Two-exposure Method

The General Electric XRD-5 diffractometer, equipped with proportional counter was used in this investigation. Copper radiation filtered by a nickel foil at 50 KV, 16 mA and a 3° beam slit, coupled with a 0.2° detector slit at $\psi = 0^\circ$, and a 0.1° detector slit at $\psi = 30^\circ$ were employed for the Cu-20 w/o Zn specimen. Chromium radiation filtered by a vanadium foil and the same diffraction conditions were employed for 6061 aluminum alloy. The specimen positioning, ψ rotation, and focusing of the detector were accomplished by employing the specimen stage and the radially-adjustable detector support as shown in Figure 15. The radial focus distance has been tabulated in Table 1 for the diffraction angles and the ψ angles that are commonly used.

A peak-to-background ratio of about 4:1 was obtained from (420) and (311) planes for Cu-20 w/o Zn and 6061 aluminum alloy, respectively. The three-point parabola method for determining peak position was used in this investigation. The three points were selected above 85% of the



Figure 13. Radially-adjustable Detector Support and Residual-stress Specimen Stage (Two Parts)



Figure 14. Uniaxial Straining Jig for X-ray Diffraction Stress Measurement Mounted on Specimen Stage, Aluminum Specimen Installed in Place



(a)



(b)

Figure 15. General Electric XRD-5 Diffractometer with Residual-stress Stage, Uniaxial Straining Jig, and Radially-adjustable Detector Support Installed: (a) $\psi = 0$, (b) $\psi = 30^\circ$

maximum intensity to minimize errors due to peak shape. For both specimens, the intensities were measured as reciprocal intensity by recording the time for 100,000 counts. In order to achieve a reasonable degree of accuracy in the X-ray measurement of stress, the Lorentz-polarization and absorption factors were applied to the values of reciprocal intensity before determining peak positions.

Stress was applied to the specimen mounted in the X-ray diffractometer, by means of the previously mentioned uniaxial straining jig. Five different stress levels were applied to each specimen from zero stress increasing to 60 percent of the yield stress. The values of applied stress were determined from SR-4 type strain gages mounted on the surface of the specimen. Stress-free annealed powder of each specimen was also investigated to obtain a correction ($\Delta 2\theta_0$) to all $\Delta 2\theta$ values measured on the stressed specimens (Cullity 1967).

In the diffractometer method the quantity that is measured is $\Delta 2\theta = (2\theta_{\perp} - 2\theta_{\psi})$, the shift in the diffraction line due to stress as the angle ψ is changed. But certain geometrical effects, especially the compromise position of the receiving slit, introduce errors which cause a slight change in 2θ even for a stress free specimen, when ψ is changed from 0° to a specific angle. It is thus important to determine this change experimentally and use it to correct all of the 2θ values measured for the stressed specimen.

4.3.2 Back-reflection Method

Due to the size of the instrument and the problem of the physical size of the specimen, a normal incidence exposure, as shown in Figure 16,

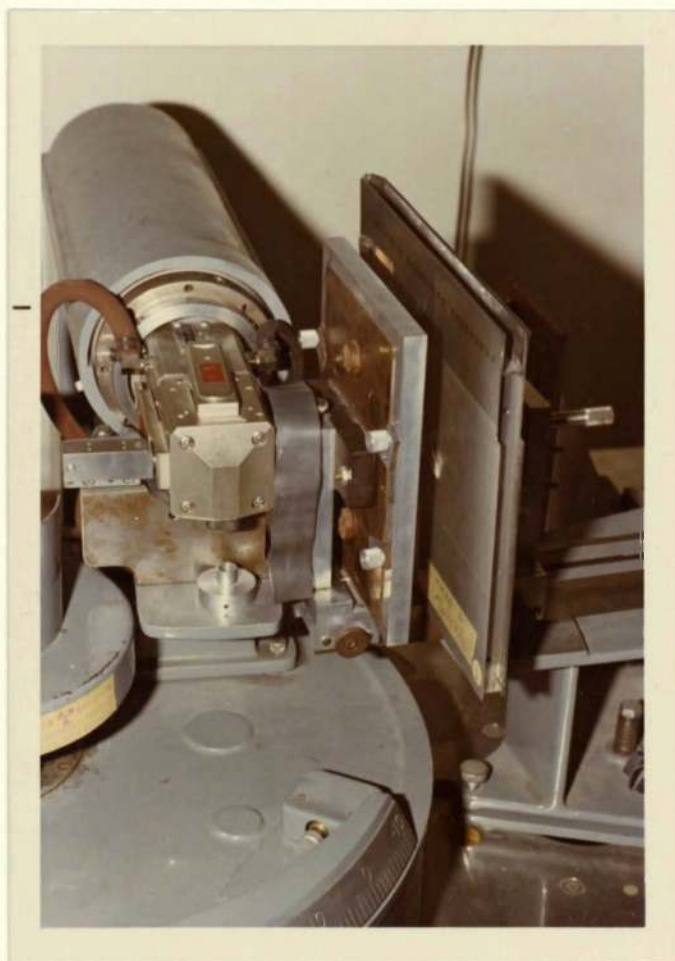


Figure 16. General Electric XRD-5 X-ray Unit with Pinhole Camera at Normal Incidence Exposure. Specimen Mounted in Position

was taken of the spot-welded assembly. The General Electric X-ray diffractometer with a high-intensity copper tube and a pinhole camera loaded with No-Screen Kodak medical X-ray film were employed in this investigation. Annealed copper powder as a standard reference material was smeared on the surface of interest of the spot-welded fin specimen. A lead cup with 0.020" hole was put on the collimator to concentrate the X-ray beams on the small welded spot area (0.045"). A stress-free area and four spot welds were selected for investigation at the approximate 3 cm. or 5 cm. specimen-to-film distance, using nickel-filtered copper K_{α} radiation at 50 KV and 24 mA and 2 hours exposure time.

The back-reflection pinhole patterns obtained are shown as Figures 17, 18, 19, 20 and 21. The Debye rings of reference material (annealed copper powder) and specimen (nickel-chromium alloy) both are from (331) reflecting planes. The patterns were measured using a traveling microscope made by W. G. PYE Company in England. On each pattern, four readings were made and averaged on the fiducial mark and on the diffraction line.

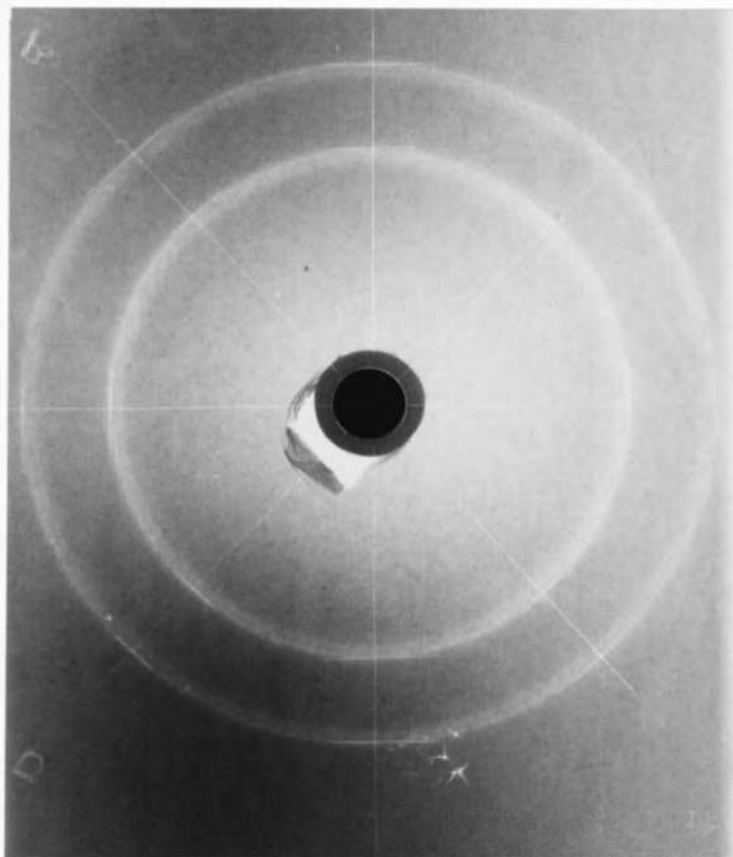


Figure 17. Back-reflection Pinhole Pattern of Spot-welded Fin Specimen (Stress-free). Specimen-to-film Distance was 5 cm

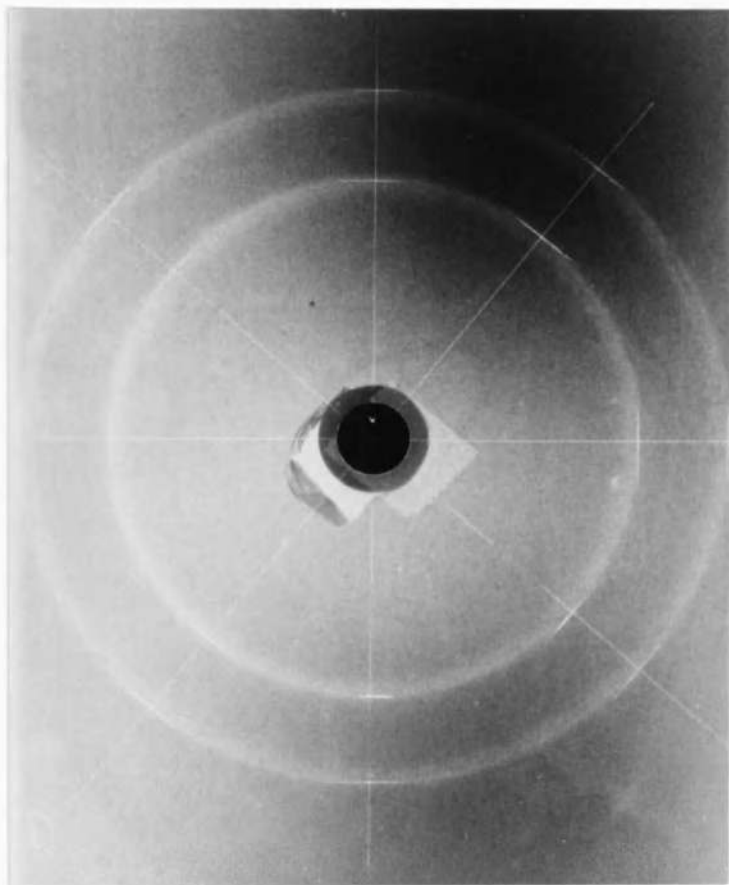


Figure 18. Back-reflection Pinhole Pattern of Welded Spot No. 1 (57400 psi). Specimen-to-film Distance was 5 cm

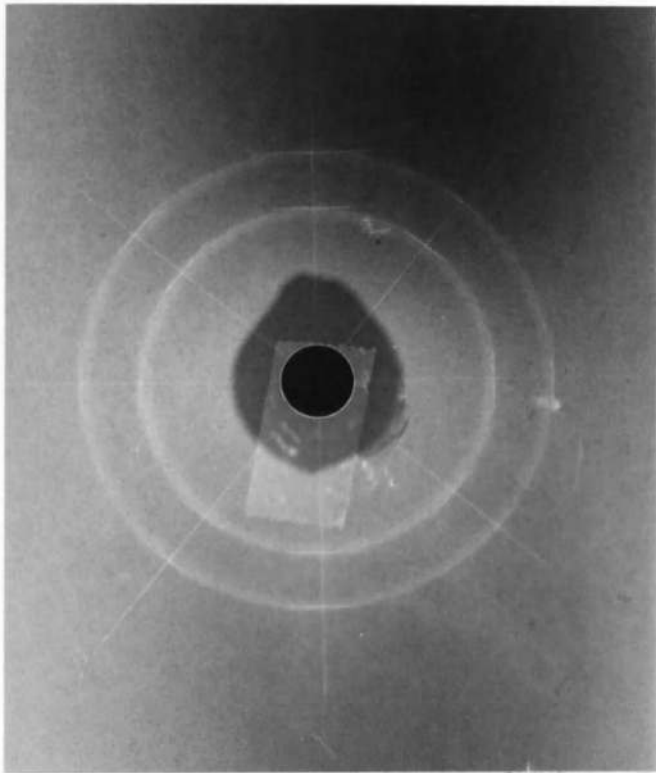


Figure 19. Back-reflection Pinhole Pattern of Welded Spot No. 2 (-11900 psi). Specimen-to-film Distance was 3 cm

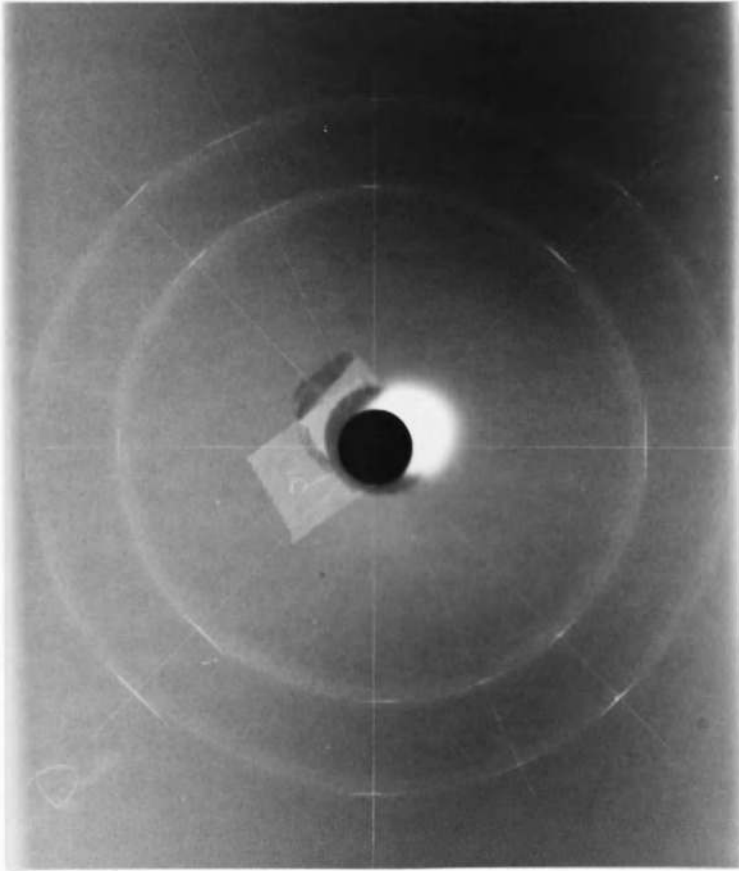


Figure 20. Back-reflection Pinhole Pattern of Welded Spot No. 3 (43000 psi). Specimen-to-film Distance was 5 cm

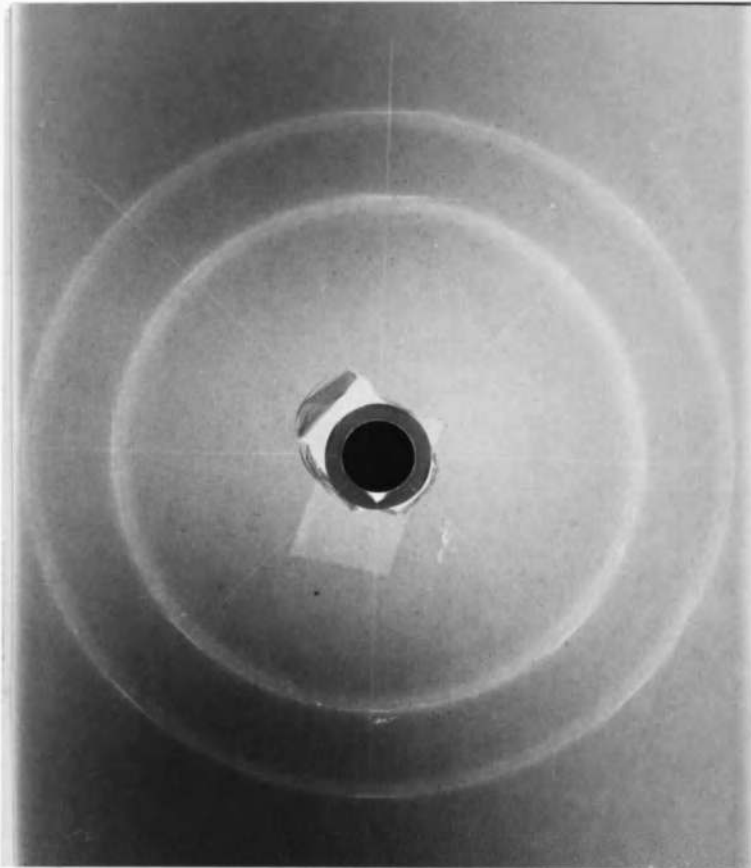


Figure 21. Back-reflection Pinhole Pattern of Welded Spot No. 4 (-1200 psi). Specimen-to-film Distance was 5 cm

CHAPTER 5

RESULTS AND DISCUSSION

5.1 Results

The peak shift or $\Delta 2\theta = (2\theta_o - 2\theta_{30})$ of 6061 aluminum alloy and Cu-20 w/o Zn measured by the three-point parabolic method with Lorentz-polarization and absorption correction factors applied are given in Table 3.

Table 3

Peak Shift for Cu-20 w/o Zn and 6061 Aluminum Alloy
Stress Determinations

Specimen	Stress, psi	$\Delta 2\theta = (2\theta_o - 2\theta_{30})$, Degrees
Cu-20 w/o Zn	0	0.176
	5100	0.213
	7700	0.244
	10250	0.256
	13000	0.280
Al-6061	0	0.091
	7600	0.182
	11500	0.213
	16500	0.273
	20500	0.320

A computer program used to convert these X-ray data into residual stress values was written by Braski and Royster (1966). The calibration curves vs peak shift, $\Delta 2\theta = (2\theta_0 - 2\theta_{30})$ were plotted in Figures 22 and 23. Straight lines were fitted to the data points by the method of least squares and displayed slopes or stress factors K of 8,410 and 13,300 psi per 0.1 degree of peak shift for 6061 aluminum alloy and Cu-20 w/o Zn, respectively. The stress factor of 6061 aluminum alloy obtained in this investigation is close to the result of 10270 psi per 0.1 degree peak shift for 5083 aluminum alloy observed by Hilley et al. (1966). The values of stress factor K of 5083 aluminum alloy observed by M. E. Hilley under various radiations, angles, and reflecting planes are shown in Table 4. It should be noted that the specific value of the stress factor K is a function of the wave length of X-rays employed, the particular set of diffracting planes, and also the specimen angle employed.

The values the sum of principal stresses of the four selected spots on the spot-welded fin specimen were calculated using the equation, $\tan(180^\circ - 2\theta) = \frac{S}{2D}$, mentioned in the section 2.3 and Equation (11). These values are 57400, 43000, -11900, and -1200 psi. The positive and negative values will be discussed in the Discussion section.

5.2 Discussion

In the measurement of residual stress by the two-exposure method, Equation (23) was employed. This equation contains a stress factor K, by which the diffraction line shift is converted to a stress value. The

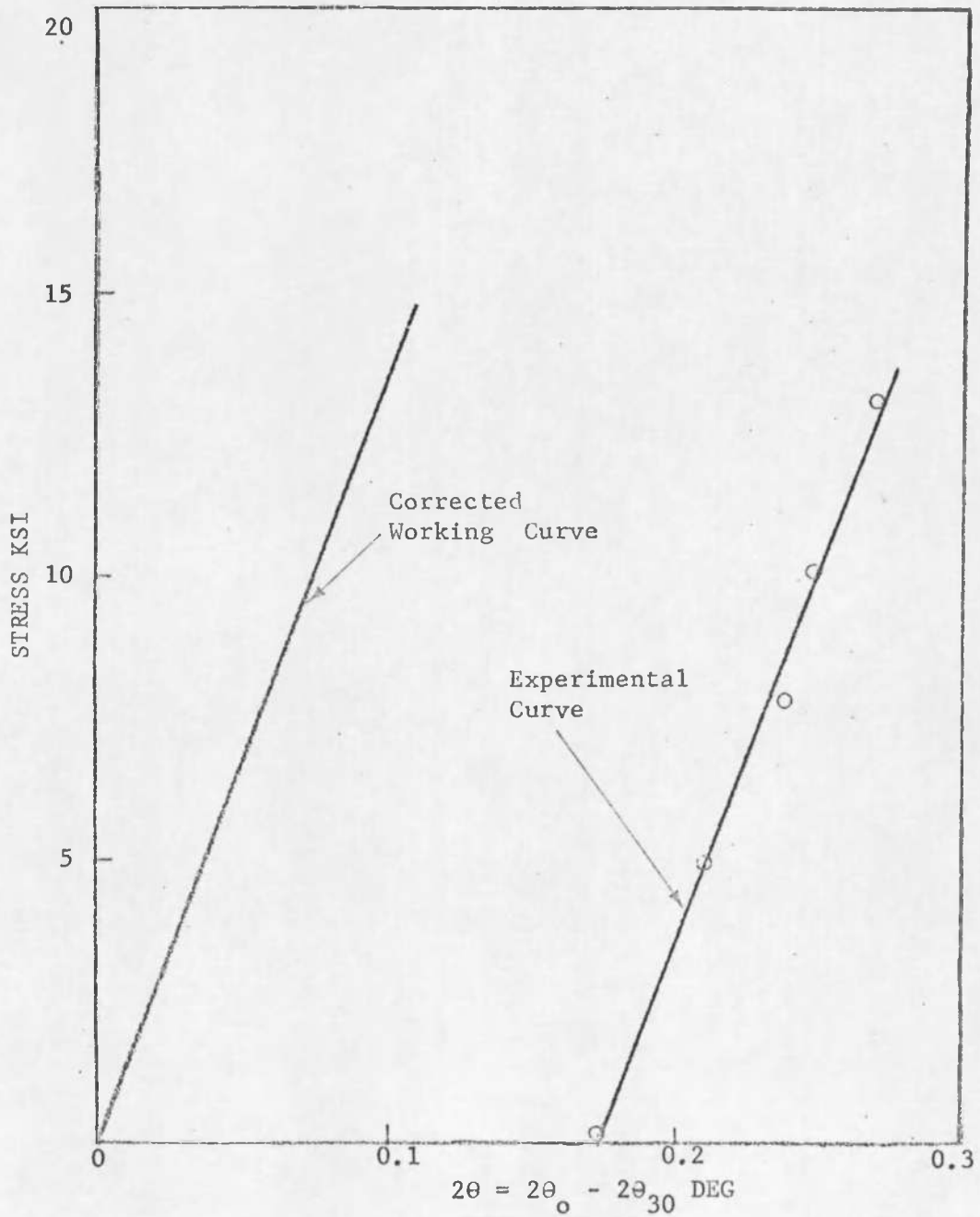


Figure 22. Data for Stress vs Peak Shift, Cu-20 w/o Zn

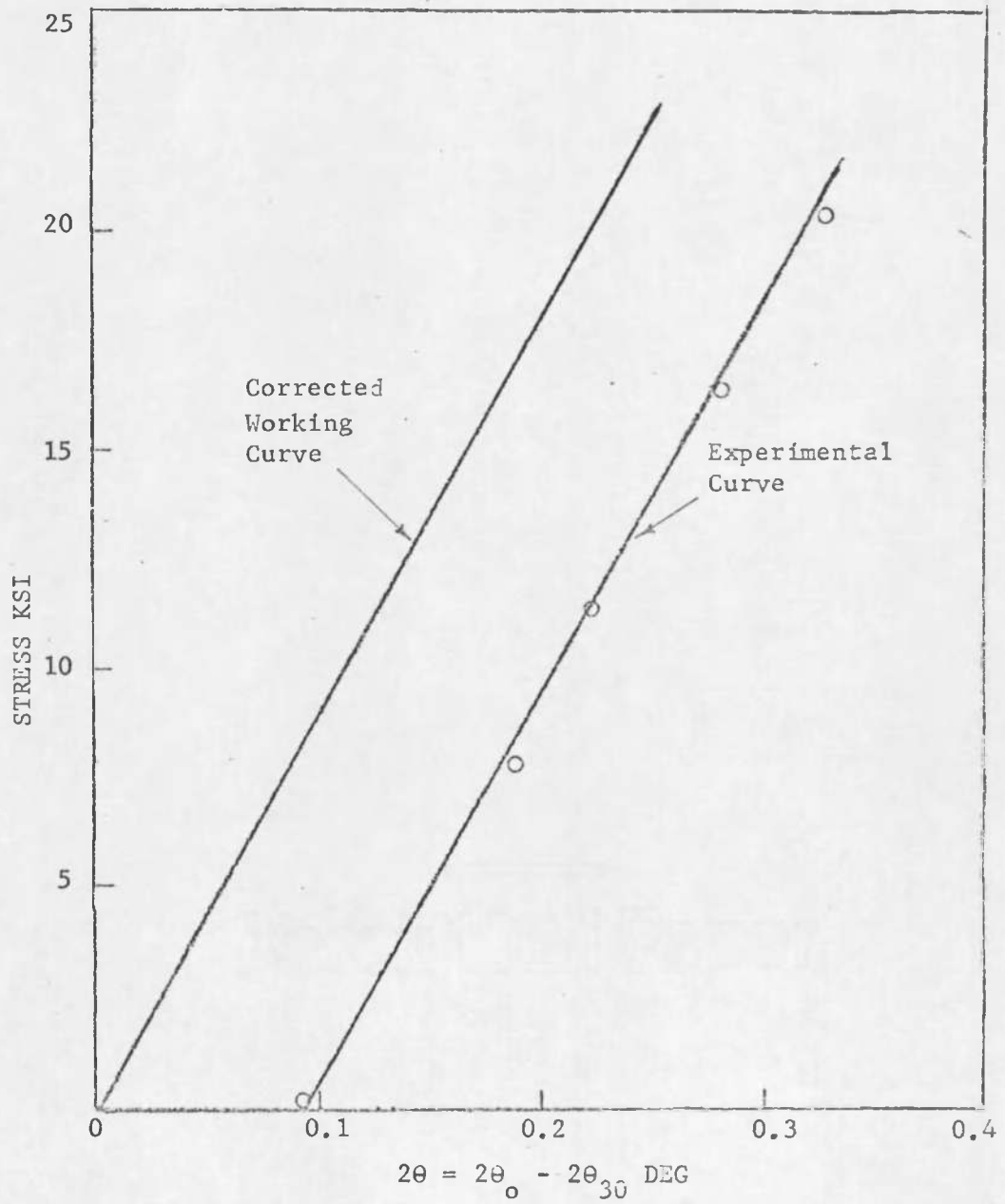


Figure 23. Data for Stress vs Peak Shift, 6061 Aluminum Alloy

Table 4

Values of Stress Factor, K , for 5083 Aluminum Alloy under Various Diffraction Conditions

X-ray target	Diffraction peak, 2θ	Specimen angle, ψ	Stress factor K , psi/0.01 deg 2θ	Radial focus, † in.
Cr*	(311) 139.5°	30	1027.31	2.75
		45	513.66	2.64
Cr	(222) 156.9°	30	568.56	4.52
		45	284.28	3.78
		60	189.52	2.73
Ce	(331) 148.9°	30	774.16	4.14
		45	387.08	3.24
		60	258.06	2.00
Co*	(420) 162.6°	30	425.73	4.80
		45	212.86	5.53
		60	141.91	3.33
Cu	(422) 137.5°	30	1081.93	3.63
		45	540.96	5.73
Cu(K_{β})*	(440) 153.0°	30	667.08	4.33
		45	333.54	3.51
		60	222.36	2.36
Cu*	(511) (333) 162.5°	30	428.20	4.79
		45	214.10	4.20
		60	142.73	3.32

* Recommended peaks.

stress factor K contains the factor $\frac{E}{1 + \nu}$, and we have tacitly assumed that the material under stress is an isotropic body obeying the laws of elasticity. However, many crystalline materials, such as iron, are not isotropic and their elastic properties vary with crystal direction. X-ray measurements are dependent on the determination of the change in lattice planar spacings of a particular set of crystallographic planes at particular orientations to the direction of stress. Therefore, the values of E and ν under these conditions may vary considerably from the bulk E and ν values mechanically measured. However, in the X-ray stress measurement, where the d or 2θ values are measured at two specific ψ angles, the difference in d or 2θ will always be proportional to the stress despite any difference in E or ν that may exist at those ψ angles. For this reason, it is advisable to determine the stress factor K experimentally by the use of electric resistance strain gages on material subjected to known stresses. For the same material the measured values of K vary with the radiation used, the rotation angles ψ , and the Miller indices of the reflecting planes.

Another contributing factor that may cause error in the evaluation of residual stress is the peak shift, $\Delta 2\theta = (2\theta_{\perp} - 2\theta_{\psi})$ due to stress as the angle ψ changed. Theoretically, the peak shift $\Delta 2\theta$ should be zero for a stress-free specimen. But in this investigation, the $\Delta 2\theta$ of 0.091 and 0.176 degree for annealed 6061 aluminum alloy and annealed Cu-20 w/o Zn powder were observed, respectively. This is due to certain geometrical effects, particularly the compromise position of the detector slit. Therefore, an amount ($\Delta 2\theta_0$), measured on the stress-free specimen must be applied to all $\Delta 2\theta$ values measured on the stressed

specimen. This is the standard method (Cullity 1967) used to calibrate the experimental values. A corrected working curve with the same slope as the experimental curve but shifted an amount ($\Delta 2\theta_0$) was applied in this investigation and shown in Figure 22 and Figure 23.

The back-reflection pinhole patterns obtained in this investigation showed smooth, continuous Debye rings. The nature of the Debye ring is critical with regard to specimen grain size. The governing effect is the number of grains which take part in the diffraction. When the grain size is quite coarse, only a few crystals diffract and Laue spots are obtained. But when the grain size is fine enough, the crystals present in the specimen, will reflect to different parts of the Debye ring. Then the smooth, continuous Debye rings are produced. Therefore, in the X-ray stress measurement a fine grain size specimen is required which makes an accurate determination of diffraction line position possible.

A schematic drawing of the profile of a typical welded spot is illustrated in Figure 24 to explain the positive and negative stress values obtained from the spots. When the portion A in the drawing is struck by the X-ray beams, a high positive stress value is obtained. This is expected, because this portion has a much smaller radius than that of portion B, a stronger tensile stress occurs. When the portion B is struck by the X-ray beams a lower negative (compression) stress value is obtained as expected.

It is important to point out that this explanation disregards the possible occurrence of thermal stresses due to the localized heating and

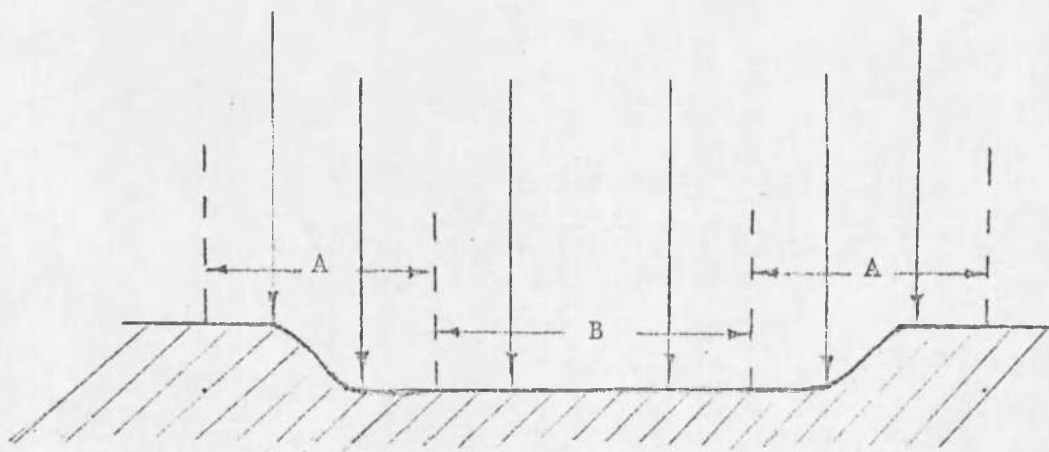


Figure 24. Schematic Drawing of Welded Spot Struck by the X-ray Beams

cooling during applied pressure which takes place in the spot-welding process. It is likely that these are the major causes of the residual stresses and the magnitude of these stresses would be expected to vary greatly from the center to the edge of the welded spot.

CHAPTER 6

CONCLUSIONS

The X-ray diffraction method is the most useful method employed for nondestructive measurement of residual stress, particularly when the stress varies rapidly over the surface of the specimen. The X-ray diffraction method is not only applicable to stress analysis at low stress levels, but also at ultrahigh stress levels (Woehrle and Reilly 1964).

The forms of Equations (23) and (25), one for the diffractometer and one for the film camera, both show that a plot of stress vs the peak shift should result in a straight-line relation. The slope of this straight line is the stress factor. Therefore, this plot may be used as the criterion to determine the validity and accuracy of the investigation. If the investigation is not valid and accurate, then a deviation from linearity will be observed. The data obtained from 6061 aluminum alloy and Cu-20 w/o Zn in the two-exposure method, show that this investigation is valid and quite accurate.

In the two-exposure method, a maximum sensitivity of stress measurement is desirable. From Equation (22), it is clear that this can be obtained by making the rotation angle ψ as large as possible, therefore reducing the $\frac{1}{\sin^2 \psi}$ term, and by selecting 2θ so as to reduce the $\cot \theta$ term. The maximum usable value of ψ is physically fixed at θ , but normally 60° is the maximum ψ value used. The value of θ is obviously a function of the material and the wave length of radiation. Therefore, the choice of the proper radiation and the diffraction planes to provide

as large a diffracting angle as possible is an important job in an investigation. Christenson has pointed out that the sensitivity of stress measurement rapidly decreases as the angle 2θ become less than 130° .

A corrected working curve with an amount ($\Delta 2\theta_0$) measured on a stress-free specimen must be employed for a reliable and accurate stress analysis.

The X-ray laboratory in the Metallurgical Engineering Department of The University of Arizona is now equipped with the necessary instrumentation for obtaining residual stress measurements on metal specimens with an accuracy comparable to that obtained in investigations reported in current literature.

LIST OF REFERENCES

- Barrett, C. S. and T. B. Massalski. Structure of Metals. 3rd Edition. New York: McGraw-Hill Publishing Co., 1966.
- Braski, D. N. and D. H. Royster. "X-Ray Measurement of Residual Stresses in Titanium Alloy Sheet," in J. B. Newkirk and G. R. Mallett (eds.) Advances in X-Ray Analysis, Vol. 10. New York: Plenum Press (1966) pp. 295-309.
- Christenson, A. L., et al. (ed.). "The Measurement of Stress by X-Ray," SAE Technical Report 182. New York: SAE, Inc., 1960.
- Cullity, B. D. Elements of X-Ray Diffraction. Reading, Mass.: Addison-Wesley Publishing Co., 1967.
- Hilley, M. E., J. J. Wert and R. S. Goodrich. "Experimental Factors Concerning X-Ray Residual Stress Measurements in High-Strength Aluminum Alloys," in J. B. Newkirk and G. R. Mallett (eds.) Advances in X-Ray Analysis. Vol. 10. New York: Plenum Press (1966) pp. 284-294.
- Koistinen, D. P. and E. Marburger. "A Simplified Procedure for Calculating Peak Position in X-Ray Residual Stress Measurements of Hardened Steel," ASM Trans., Vol. 51 (1959) p. 537.
- Norton, J. T. "X-Ray Stress Measurement by the Single-Exposure Technique," in J. B. Newkirk and G. R. Mallett (eds.) Advances in X-Ray Analysis. Vol. 11. New York: Plenum Press, 1968.
- Ogilvie, R. E. "Stress Measurement with X-Ray Spectrometer," Master's Thesis, MIT, 1952.
- Timoshenko, S. P. Theory of Elasticity. New York: McGraw-Hill Book Co., 1936.
- Woehrle, H. R. and F. P. Reilly. "Experiment X-Ray Stress Analysis Procedures for Ultrahigh-Strength Materials," in W. M. Mueller, G. R. Mallett and M. J. Fay (eds.) Advances in X-Ray Analysis. Vol. 8. New York: Plenum Press (1964) pp. 38-47.

